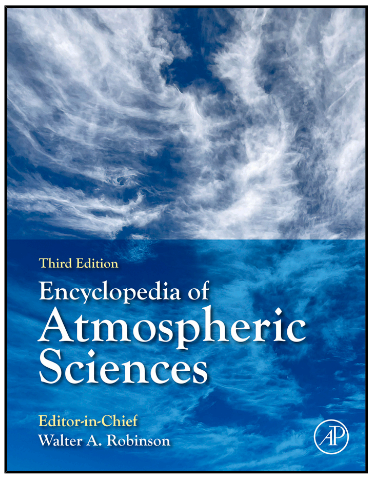

Meng, Z., Zhang, F., Zhang, Y., 2026. Ensemble-Based Data Assimilation. In: Robinson, W.A. (Ed.), Encyclopedia of Atmospheric Sciences, vol. 1. Elsevier, Academic Press, pp. 139–147. https://dx.doi.org/10.1016/B978-0-323-96026-7.00027-8.
ISBN: 9780323960267

Ensemble-Based Data Assimilation

Z. Meng[a], **F. Zhang**[†], **and Y. Zhang**[b], [a] Peking University, Beijing, China; and [b] Pennsylvania State University, University Park, State College, PA, United States

This is an update of Z. Meng, F. Zhang, DATA ASSIMILATION AND PREDICTABILITY | Ensemble-Based Data Assimilation, Editor(s): Gerald R. North, John Pyle, Fuqing Zhang, Encyclopedia of Atmospheric Sciences (Second Edition), Academic Press, 2015, Pages 241–247, ISBN 9780123822253, https://doi.org/10.1016/B978-0-12-382225-3.00495-3.

Key Points

- This article introduces the concepts, formulations, advantages, deficiencies, practical considerations, and applications of ensemble-based data assimilation (EDA) techniques.
- EDA such as the ensemble Kalman filter (EnKF) is widely used in research and operational communities using regional and global numerical weather prediction models.
- The limited ensemble size in current EDA applications leads to rank deficiency and sampling errors, which are often treated by inflation and covariance localization.

Synopsis

This article introduces the algorithm of ensemble-based data assimilation (EDA) and the main issues in its application to atmospheric sciences. EDA is drawing increasing attention in data assimilation community mainly due to its flow-dependent background error covariance determined using a short-range ensemble forecast and ease of implementation. Many types of EDA have been applied with different models at different scales in both research and operational or quasi-operational communities. Various aspects involved in EDA are discussed including observations, ensemble initialization, sampling error, covariance inflation and localization, model error, verification, nonlinearity and non-Gaussian errors, intercomparison, and hybrid with variational schemes.

Introduction

The accuracy of weather forecasts is mainly determined by the accuracy of numerical weather prediction (NWP). NWP produces the time evolution of basic meteorological variables including wind, pressure, temperature, moisture, and other hydrometeors based on basic physical laws. Its accuracy depends critically on the qualities of the initial conditions and the forecast model. The initial conditions of an NWP model are usually produced through data assimilation, a procedure that aims to estimate the state and uncertainty of the atmosphere as accurately as possible by combining all available information (including both previous model forecasts and current observations, and their respective uncertainties). Data assimilation methods update the model forecasts through the error covariance of the model forecast between different grid points and variables.

Data assimilation is typically performed through one of the two methods. The first method is variational method, which finds an analysis that has a minimum misfit to the observation and the background forecast (or the first guess). Two main methods in this

[†]Deceased

Encyclopedia of Atmospheric Sciences, Third Edition, 2026, 139–147

category are three-dimensional (3DVar, three dimensions in terms of space, Barker et al., 2004) and four-dimensional variational methods (4DVar, three dimensions in terms of space plus one in terms of time, Le Dimet, 1982). Variational methods generally produce their background error covariance using a period of forecast differences between different lead times (Barker et al., 2004; Xiao and Sun, 2007), thus is isotropic and stationary.

The other approach is sequential data assimilation. A theoretically optimum sequential method is the Kalman filter, which assumes Gaussian errors and a linear system. Kalman filter is named as extended Kalman filter for nonlinear models. Since the extended Kalman filter explicitly propagates the background error covariance, it is not practical for large-dimensional systems like the atmosphere or the ocean. Evensen (1994) proposed the ensemble Kalman filter (EnKF) that estimates the background error covariance with a short-term ensemble forecast. The EnKF is drawing increasing attention in data assimilation community. Since its first application in atmospheric sciences (Houtekamer and Mitchell, 1998), many types of EnKFs have been applied with different models at different scales (Lorenc, 2003; Houtekamer and Mitchell, 2005; Hamill, 2006; Ehrendorfer, 2007; Meng and Zhang, 2010). The potential of using ensemble-based data assimilation (EDA) is also being explored in several operational meteorological centers, and many EDA systems for global models or limited area models (LAM) are now running operationally or quasi-operationally. This article aims to give a brief introduction to the EnKF algorithm and main issues in its application to atmospheric sciences. For a more comprehensive overview, the readers are referred to Houtekamer and Zhang (2016).

The Concept of the EnKF

The EnKF has two steps: an analysis step and a forecast step (Fig. 1). The analysis step in the standard EnKF proceeds according to the classical Kalman filter equations with the required sample means and covariances:

$$\mathbf{x}_\mathbf{i}^\mathbf{a} = \mathbf{x}_\mathbf{i}^\mathbf{b} + \mathbf{K}\left(\mathbf{y}_\mathbf{i}^\mathbf{o} - H\mathbf{x}_\mathbf{i}^\mathbf{b}\right), \text{for } \mathbf{i} = 1, \ldots, n \tag{1}$$

$$\mathbf{K} = \mathbf{P}^\mathbf{b}\mathbf{H}^\mathbf{T}\left(\mathbf{H}\mathbf{P}^\mathbf{b}\mathbf{H}^\mathbf{T} + \mathbf{R}\right)^{-1} \tag{2}$$

$$\mathbf{P}^\mathbf{b} = \frac{1}{n-1}\sum_{\mathbf{i}=1}^{n}\left[\left(\mathbf{x}_\mathbf{i}^\mathbf{b} - \overline{\mathbf{x}^\mathbf{b}}\right)\left(\mathbf{x}_\mathbf{i}^\mathbf{b} - \overline{\mathbf{x}^\mathbf{b}}\right)^\mathbf{T}\right] \tag{3}$$

$$\mathbf{P}^\mathbf{a} = \frac{1}{n-1}\sum_{\mathbf{i}=1}^{\mathbf{n}}\left[\left(\mathbf{x}_\mathbf{i}^\mathbf{a} - \overline{\mathbf{x}^\mathbf{a}}\right)\left(\mathbf{x}_\mathbf{i}^\mathbf{a} - \overline{\mathbf{x}^\mathbf{a}}\right)^\mathbf{T}\right] \tag{4}$$

where, $\overline{\mathbf{x}^\mathbf{b}}$ and $\overline{\mathbf{x}^\mathbf{a}}$ are the sample mean values of the forecast and the analysis ensemble. The analysis state vector, $\mathbf{x}_\mathbf{i}^\mathbf{a}$ for the $\mathbf{i}$th ensemble member is obtained by adding to the background state vector, $\mathbf{x}_\mathbf{i}^\mathbf{b}$, a weighted difference between observations, $\mathbf{y}^\mathbf{o}$, and the background state vector projected to observation space through an observation operator, H. $\mathbf{P}^\mathbf{a}$ and $\mathbf{P}^\mathbf{b}$ are the analysis and background error covariance respectively, which are approximated in the EnKF by the respective ensemble covariance. $\mathbf{K}$ is the Kalman gain, which takes into account the observation error, $\mathbf{R}$, and the background error covariance, $\mathbf{P}^\mathbf{b}$ in determining the extent to which observations are weighted relative to the background. $\mathbf{H}$ and $\mathbf{H}^\mathbf{T}$ are the tangent linear and adjoint versions of H, respectively. Tangent linear means the linearization about a time or space-varying trajectory of a nonlinear operator, which gives the evolution of the first-order perturbation of a nonlinear vector. In the EnKF, $\mathbf{P}^\mathbf{b}\mathbf{H}^\mathbf{T}$ and $\mathbf{H}\mathbf{P}^\mathbf{b}\mathbf{H}^\mathbf{T}$ are calculated using the sample covariance and thus $\mathbf{H}^\mathbf{T}$ and $\mathbf{H}$ are not explicitly needed.

Given the analysis ensemble, the forecast step simply involves forecasting each member forward from time t to $t + \Delta t$ when the next observations are available:

$$\mathbf{x}_\mathbf{i}^\mathbf{b}(t + \Delta t) = M\left(\mathbf{x}_\mathbf{i}^\mathbf{a}(t)\right), \text{for } \mathbf{i} = 1, \ldots, n \tag{5}$$

where M is a nonlinear model. The ensemble-based algorithm asymptotically approaches the Kalman filter in the limit of a large ensemble and Gaussian error distributions.

The EnKF has many variants. Based on the method for generating the analysis ensemble, an EnKF can be characterized as stochastic, where the analysis ensemble is obtained with the Kalman gain and randomly perturbed observations, or deterministic, where the analysis ensemble is created by transforming the forecast ensemble without perturbing the observations. Due to the large

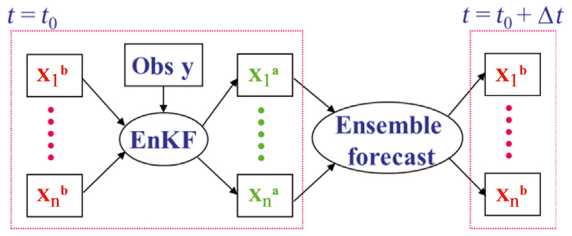

Fig. 1 Schematic diagram of the flow chart of the EnKF. The meaning of the various variables is referred to the text. EnKF, ensemble Kalman filter.

dimension of the model state vector and the large number of observations needed in the LAM-EnKF scenario, various algorithms of the LAM EnKF have been proposed to improve computational efficiency. The most commonly employed deterministic method has the form of ensemble square root filters (EnSRFs) such as the serial EnSRF, the ensemble transform Kalman filter (ETKF), and the ensemble adjustment Kalman filter (EAKF).

Observations

Different observing platforms or different formulations of the same observations may have different impacts on the EnKF performance. For example, radiosonde observations have been found to have the largest impact on regional-scale analyses and forecasts. Due to errors coming from the difference between the real and the model terrain height and uncertainties in the parameterization of boundary layer and land surface physical processes, surface observations have been a big challenge. The analysis and forecast error may benefit from removing the bias and reducing the representativeness error by assimilating only those data whose locations have a terrain height that matches the model one, and removing the bias of surface wind and temperature before assimilation. However, surface data assimilation may have very limited impact on the levels above the surface and on the time length of the forecast into the integration.

Besides the conventional radiosonde and surface observations, remotely sensed observations are drawing more and more attention. Doppler radars such as Doppler on Wheels, Weather Surveillance Radar 88 Doppler, and airborne radars have sufficient temporal and spatial coverage to fully observe convective clouds. The effectiveness of using the EnKF to assimilate Doppler radar velocities for supercell storms was first demonstrated in Snyder and Zhang (2003) and with real-data in Dowell et al. (2004). An X-band radar network that was deployed by the National Science Foundation Engineering Research Center for Collaborative Adaptive Sensing of the Atmosphere has been helpful in improving the analysis and forecast of convective system, which supports convective-scale warn-on-forecast operations. Airborne Doppler radar radial-velocity observations have also been successfully assimilated in real time for a hurricane prediction model (Zhang et al., 2011). The EnKF system has demonstrated promising performance, especially on hurricane intensity forecasts, through experiments over 61 applicable The National Oceanic and Atmospheric Administration (NOAA) P-3 airborne Doppler missions during the 2008−10 Atlantic hurricane seasons (**Fig. 2**). The mean absolute intensity forecast errors initialized with the EnKF analysis of the airborne Doppler velocities at the 24−120-h lead forecast times were 20%−40% lower than the National Hurricane Center's official forecasts issued at similar times. Radar reflectivity has been shown to be less effective than Doppler radial velocity. The likely non-Gaussian error distribution, weak cross-correlations between state variables, inherent small-scale variability, and strong dependence of these quantities on the accuracy of model microphysics schemes appear to be the main limiting factors. Nevertheless, the assimilation of differential reflectivity, Z_{dr}, reflectivity difference, Z_{dp}, and specific differential phase, K_{dp}, beyond radar reflectivity and/or radial velocity may improve storm analysis (Jung et al., 2008). Moreover, the assimilation of even the echo-free radar observations, defined as radar reflectivity below a threshold value of 5 d*BZ*, sometimes may effectively suppress spurious convection (Aksoy et al., 2009).

Radar data need to be vigorously preprocessed to have a consistently positive impact. With large volumes of radar observations recorded at a much higher resolution than the forecast model grid spacing, significant data thinning may be necessary. The process of combining multiple observations into one high-accuracy 'super' observation is often referred to as 'superobbing.' This data preprocessing procedure has been implemented operationally on the NOAA hurricane reconnaissance aircraft that allows for more efficient real-time transmission of airborne radar observations to the ground (Zhang et al., 2011). Assimilating airborne Doppler radar data in storm-relative coordinates under a simultaneity assumption may produce a better kinematic tropical cyclone (TC) structure and a slower error growth (Aksoy, 2013). This method translates the observations of the whole flight to a common storm center by maintaining their relative positions at the time of their actual sampling, then randomly distributed to different cycles to achieve a more homogeneous data coverage among data assimilation cycles. Many recent studies are also using EDA to assimilate the observation products generated by the dual-polarization radars (e.g., Putnam et al., 2021) and high-frequency (every 30 to 60 seconds) observations generated by the phased-array radars (PAR; e.g., Stratman et al., 2020; Wang et al., 2021; Honda et al., 2022).

In addition to radars, the assimilation of satellite observations and/or satellite-derived products is also a hot topic. Multivariate specific humidity retrieved from the Atmospheric Infrared Sounder (AIRS), satellite-derived atmospheric motion vectors, and temperature and mixing ratio profiles derived from the AIRS instrument on board the *Aqua* satellite have been shown beneficial for weather analysis and forecast (Jones and Stensrud, 2012). Many recent studies focus on the direct assimilation of satellite radiance using EnKF or EDA, with emphasis on the 'all-sky' approach that assimilates radiance both from the clear-sky conditions and impacted by clouds and precipitation. Cases studies and systematic evaluations show that assimilating all-sky infrared radiance from new-generation geostationary satellites leads to improved forecasts for tropical and extratropical cyclones, thunderstorms, mesoscale convective systems, and convective cells. Zhang et al. (2021) reported improved track, intensity, and precipitation forecasts of Hurricane Harvey with the assimilation of all-sky microwave radiance from the constellation sensors of the Global Precipitation Measurement (GPM) satellites using EnKF. The recent development of advanced statistical methods, including machine learning (ML) and artificial intelligence (AI) techniques, also have great potentials to help the assimilation of satellite radiance, such as constructing observation operators that are much faster than the traditional radiative transfer models, or channel selection and dimension reduction for the hyperspectral infrared sounders. However, many issues remain to be explored in satellite radiance assimilation such as observation bias correction, observation error modeling, and channel selection and combination.

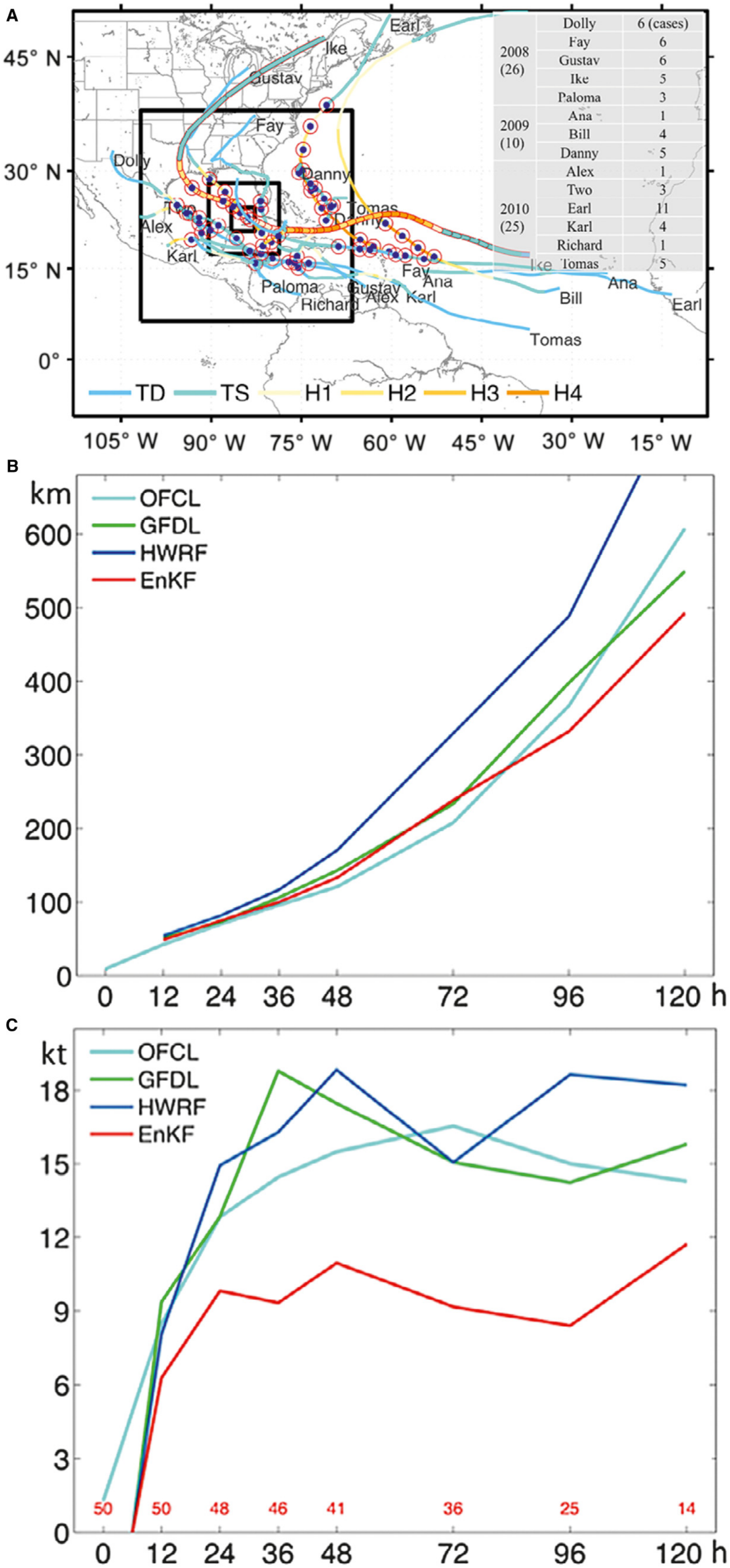
A
45° N
30° N
15° N
0°
105° W
90° W
75° W
60° W
45° W
30° W
15° W
2008 (26)
2009 (10)
2010 (25)
Dolly 6 (cases)
Fay 6
Gustav 6
Ike 5
Paloma 3
Ana 1
Bill 4
Danny 5
Alex 1
Two 3
Earl 11
Karl 4
Richard 1
Tomas 5
Earl
Ike
Gustav
Fay
Dolly
Danny
Tomas
Alex
Karl
Paloma
Richard
Ana
Bill
TD
TS
H1
H2
H3
H4
B
km
OFCL
GFDL
HWRF
EnKF
0
100
200
300
400
500
600
0
12
24
36
48
72
96
120 h
C
kt
OFCL
GFDL
HWRF
EnKF
0
3
6
9
12
15
18
50
50
48
46
41
36
25
14
0
12
24
36
48
72
96
120 h

Besides the aforementioned *in situ* and remotely sensed data, some special synthesized object-oriented observations, such as the vortex position of tropical cyclones, can also be easily assimilated by the EnKF and have been demonstrated to be helpful in improving hurricane forecast ability.

Ensemble Initialization

How to create an initial ensemble that reflects the uncertainty of the initial analysis is an important and critical issue. Global EnKFs typically use random samples from a climatological error distribution, or generate perturbations from a preexisting 3D/4DVar system. The LAM-based EnKF may be initialized from an existing global or larger scale ensemble or by using one of the methods used for the global model if a global ensemble forecast is not readily accessible. The generation of the initial ensemble for convective-scale EnKF systems remains an open question due to the lack of accurate error statistics. For many convective-scale applications, Gaussian noises are added to a horizontally uniform background (sounding) for all state variables (e.g., Snyder and Zhang, 2003).

Compared to the initial condition uncertainties, a proper representation of boundary uncertainties may have a larger impact on the LAM EnKF. A lack of sufficient ensemble spread on the lateral boundaries may propagate inward and lead to filter divergence. Filter divergence means that the ensemble mean deviates further and further away from the truth due to the underestimated variance of the forecast ensemble, which results in more weight being given to the prior (model forecast) than to the observations. Boundary perturbations can be generated using the same methods as ensemble initialization described above.

Sampling Error, Covariance Inflation, and Localization

Due to computational constraints, only a limited ensemble size can be afforded in the EnKF, which will result in sampling errors. The number of members sufficient for the EnKF to minimize the impact of sampling errors still remains an open question. Until now, most published EnKF studies use an ensemble size of 30−100, while studies show that an ensemble size of O (1000) is likely needed to accurately estimate covariances (e.g., Miyoshi et al., 2014). Due to the limited ensemble size, the EnKF generically suffers from a rank-deficiency problem in which only a part of the phase space can be spanned by the ensemble. As a result, the ensemble spread tends to be systematically underestimated.

The underestimation of ensemble spread is commonly treated by covariance inflation through multiplicative or additive scaling, or covariance relaxation. Additive covariance inflation adds a set of ensemble perturbations that can reflect forecast uncertainty to the forecast ensemble, where multiplicative covariance inflation is achieved by multiplying all ensemble perturbations before or after the EnKF analysis with a constant slightly larger than 1. However, multiplicative covariance inflation with a spatially constant inflation factor may cause a model to become unstable due to excessive spread in data-sparse regions. A Bayesian algorithm was proposed using a spatially and temporally varying adaptive inflation factor for each element of the model state vector (Anderson, 2009). Another approach is the covariance relaxation method through relaxation of the final analysis perturbations to the prior forecast (Zhang et al., 2004). The relaxation method only inflates the variance at grid points that are updated by observations, thus avoiding the overinflation deficiency of the conventional inflation method.

Besides the underestimation of ensemble spread, sampling errors in the EnKF may also cause unphysical, distant correlations and subsequently spurious analysis increments. The most commonly used approach for reducing distant spurious correlations is through covariance localization. Covariance localization is often implemented by multiplying a Gaussian shape function that decreases smoothly from one at the observation point to zero at a certain distance from the observation. The impact of an observation is thus confined only within a limited distance. This distance is usually called the radius of influence (ROI). Localization may not only decrease spurious distant correlation, but also reduce the computational cost and alleviate the rank-deficiency problem due to the limited ensemble size. The value of ROI may depend on ensemble size, observation type and density, model error and resolution, as well as the characteristic scales of the underlying dynamic system. For examples, a horizontal ROI of 1000−2000 (60−150) km is often used for standard radiosonde (surface) observations, while a much smaller ROI ranging from several to hundreds of kilometers is often used for radar observations. It was once suggested that the ROI should be two to three times the

Fig. 2 (A) The Weather Research and Forecasting model (WRF) model domain configuration and TC tracks with NOAA airborne Doppler radar mission. The outer domain is fixed for all cases, while the three inner domains are centered at the storm's center at the initial time and movable flowing model vortex center during the forecast. Fourteen storm tracks are colorized lines with storm intensity. With blue dots circled with red, 61 missions of NOAA airborne Doppler radar observation are marked. All the storms and case numbers are listed on the right top. Also shown are the mean absolute forecast error averaged over 50 samples homogenized by all 61 airborne Doppler missions during 2008−10 for The National Hurricane Center (NHC) OFfiCial forecast ('OFCL,' solid cyan line), The Geophysical Fluid Dynamics Laboratory (GFDL) hurricane model ('GFDL,' green line), The Hurricane Weather Research and Forecasting model ('HWRF,' dark blue line), and the WRF deterministic forecast in 4.5-km resolution initialized with EnKF analysis ('EnKF,' red line) after making the samples homogeneous for all five forecasts for (B) the track position error (km) and (C) the 10-m maximum wind speed error (knots) with simple bias correction for all forecasts except for OFCL. The red numbers on the x axis of (C) indicate the sample size for the homogeneous comparison. Adapted from Zhang, F., Weng, Y., Gamache, J.F., Marks, F.D., 2011. Performance of convection permitting hurricane initialization and prediction during 2008−2010 with ensemble data assimilation of inner-core airborne Doppler radar observations. Geophys. Res. Lett. 38, L15810. https://doi.org/10.1029/2011GL048469.

forecast error scales (Lorenc, 2003). Zhang et al. (2009a) proposed a successive covariance localization (SCL) technique in which a larger ROI is used to assimilate a relatively small subset of observations in the coarser domains, while a smaller ROI is used to assimilate higher density observations in the inner domains. They found clear advantages of using the SCL method over using single ROIs in the assimilation of dense radar observations for rapidly developing landfalling hurricanes. The vertical ROI is sometimes set to the depth of the atmospheric model for conventional observation assimilation or vertical covariance localization is not performed at all. Besides ROI, the selection of a covariance localization function may also be important. The most widely used covariance localization is the fifth-order correlation function of Gaspari and Cohn (1999). The choice of localization function may become more complicated for observations that have complex spatial, temporal, and physical attributes or with an unknown relation with the state variable.

While accounting for sampling error, covariance localization may cause imbalance when one observation is selected to update the state vector at one grid point, but not selected for a neighboring grid point (Lorenc, 2003). Consequently, covariance localization may produce analyses with weaker flow balance and stronger divergence, which may result in inaccurately balanced background error statistics. Methods used to reduce imbalance in large-scale models such as applying a digital filter (e.g., Lynch and Huang, 1992) or covariance localization performed in the stream function−velocity potential rather than the wind component space (Kepert, 2009).

Model Error

Since the EnKF depends critically on the quality of the first guess and the forecast error covariance estimated from a short-term ensemble forecast, the presence of model error may lead to poor filter performance and even filter divergence. Model error can result from inadequate parameterizations of subgrid-scale physical processes, numerical inaccuracy, truncation error, ill-defined boundary conditions, or other random errors. The presence of model error often results in both a large bias in the ensemble mean and too little spread, which may ultimately cause the ensemble forecast to fail.

There are several ad hoc approaches that have been used to account for model error in the context of the EnKF such as covariance inflation, bias correction, the use of multimodel or multiphysics ensemble, and simultaneous state and parameter estimation. Additive covariance inflation has been shown to be effective in improving the performance of the EnKF. Though most statistical data assimilation methods assume that the model forecast (or first guess) is unbiased, this is rarely the case. Over the past decade, there has been an increasing amount of evidence demonstrating the advantages and effectiveness of using multimodel ensembles (over single-model ensembles) to account for model error in the prediction system (e.g., Krishnamurti et al., 1999; Weisheimer et al., 2009). However, given technical implementation difficulties associated with inherent differences in model numerics, dynamical coordinates, and/or (prognostic) state variables among different forecast models, multimodel ensembles have not been used for the EnKF. Since a considerable part of the model error comes from the parameterization of subgrid-scale physical processes, a more practical approach is to use a variety of physical parameterization schemes available in the same forecast model or a variety of values of some parameters in a particular scheme for different members to account for model uncertainties. This multiphysics ensemble approach has been shown to be effective in accounting for model error in both global and mesoscale ensemble forecast systems (Meng and Zhang, 2007; Fujita et al., 2007), likely through improved ensemble mean estimates, an increased ensemble spread, and a more effective background error covariance. With the development of more sophisticated physical schemes, how to assign weights of various available schemes in the ensemble may become a critical issue. Besides, stochastic kinetic energy backscatter (Shutts, 2005) has been used as more physically based parameterization of model error (Leutbecher et al., 2007).

The uncertainty in physical parameterization schemes is closely related to the uncertainty of its parameters. Almost all parameters of subgrid physical parameterization schemes are empirical, due to a lack of direct observations, and could therefore have large and unknown uncertainties. Parameter estimation is a technique in which the EnKF is used to estimate these parameters by treating them as additional model variables and updating them through data assimilation. This technique may help improve the performance of the EnKF via a model error correction. Since there are no direct observations or physical evidence describing the variability of various parameters, the generation of a realistic initial ensemble for the estimated parameter is even more difficult than for standard state variables. Furthermore, not all parameters can be successfully estimated. The performance of a parameter estimation algorithm depends on the correlation between the parameter and model variables and is closely related to the EnKF configuration. Parameter estimation performance using the EnKF is also closely associated with the number of simultaneously estimated parameters. It was found that the estimation of a single parameter is very effective in improving the performance of the EnKF. Increasing the number of estimated parameters inevitably leads to a decline in the improvement from parameter estimation (Aksoy et al., 2006).

Verification

The realism of the analysis and forecast ensembles is usually verified using rank histogram (Anderson, 1996; Hamill and Colucci, 1997). A rank histogram describes the extent to which an ensemble encompasses the verifying data by ranking the verifying data in the sorted ensemble. The reliability of an ensemble can be diagnosed by the shape of its rank histogram. A flat shape implies that the observation can be taken as a random member of the ensemble, and consequently the ensemble is reliable. A U-shape suggests that the ensemble spread is insufficient, while a reversed (upside down) U-shape indicates that the ensemble spread is too large.

Grid point−based root mean square error (RMSE) of different variables integrated over the whole model domain is usually used for verification for the analysis and/or forecast ensemble means of the EnKF. Due to a lack of dense, conventional mesoscale observations, verification of the LAM EnKF can be more difficult than verification of larger scale prediction systems, especially for radar data assimilation. One way is to compare the analysis and/or forecast against radar observations that are not assimilated, but saved specifically for assessment. The equitable threat score can be used to verify the result in terms of radar reflectivity. An alternative metric that is more pattern-based is the reflectivity correlation coefficient between the observed and simulated reflectivity in observation space. For severe weather systems, such as hurricanes, how to choose an appropriate error metric is still an open question. Since a small displacement of a storm center may result in a substantially large RMSE of wind, performance could be better assessed using feature-based verification.

Nonlinearity and Non-Gaussian Errors

Though the EnKF can be used in nonlinear and non-Gaussian systems, the performance of the EnKF may be affected and ultimately limited by these two characteristics. Variants of algorithms for highly nonlinear and non-Gaussian systems have been proposed, such as the particle filter and its variants, the particle Kalman filter, the iterative EnKF and extended Kalman filter, the bi-Gaussian EnKF, the quantile-conserving ensemble filters, morphing methods, 'Running in place,' and the 'quasi-outer loop.' While the majority of these methods have only been applied for simple models, some algorithms have been adapted for high-dimensional systems, including research and operational numerical models, with promising results. However, how to construct proper algorithms to deal with high nonlinearity and non-Gaussianity in an efficient manner awaits further efforts.

Intercomparison and Hybrid With Variational Schemes

Despite many of the challenging issues discussed in the previous sections, there are several appealing advantages of the EnKF in comparison to the variational data assimilation techniques. These advantages include: (1) The background error covariance is flow-dependent, which reflects the errors of the day; (2) The model and observation operator can be nonlinear; (3) It provides not only the best estimation of the state, but also the associated flow-dependent uncertainty; therefore, it can be seamlessly coupled with ensemble forecasting; (4) There is no need to code a tangent linear or adjoint model; (5) It is easier to account for model error due to its use of an ensemble forecast; and (6) The ensemble members can be run simultaneously, making it easy to parallelize.

Many studies have shown that the EnKF generally compares favorably with 3DVar (Meng and Zhang, 2008a, 2008b) and 4DVar (Caya et al., 2005). Zhang et al. (2013) found that the advantage of the EnKF over both 3DVar and 4DVar becomes increasingly more after 36-h forecast time for all prognostic variables, while the EnKF moisture forecast field is superior to both 3DVar and 4DVar at all lead times despite fitting less closely to the observations at the analysis time.

Both the EnKF and variational method have their own advantages and disadvantages. The EnKF benefits from its flow-dependent background error covariance but suffers from rank deficiency, while the variational technique has advantages in its analysis algorithm. The variational approach can more efficiently assimilate large numbers of observations and apply physical constraints on the solution when minimizing the cost function, however, it is limited by the use of a static background error covariance matrix. Instead of settling on one particular method, more and more efforts are devoted to the hybridization of the two approaches. A two-way coupled assimilation scheme benefits from using the state-dependent uncertainty provided by the EnKF, while taking advantage of the variational method from data assimilation algorithm. The EnKF/3DVar hybrid system of The Global Forecasting System (GFS)/The National Centers for Environmental Prediction (NCEP) has been showing consistently better TC track forecast than the operational Gridpoint Statistical Interpolation. A hybrid of EnKF with 4DVar is regarded as one of the most advanced and most promising (as well as most computationally and technically demanding) data assimilation methods in both the research and operational communities. Zhang et al. (2013) demonstrated that EnKF/4DVar produced considerable improvements over EnKF/3DVar at forecast lead times of 1−2 days before they converged to similar results at longer lead times (**Fig. 3**). Both EnKF/3DVar and EnKF/4DVar produced considerably better forecast than stand-alone 3DVar and 4DVar methods that relied solely on static background error covariance.

It is important to bear in mind that a hybrid system will likely inherit issues or complexity from the component systems such as the rank-deficiency problem in the EnKF and the use of an outer loop in 4DVar. More efforts are needed to tackle these issues in the future. Considering the encouraging results obtained by coupling the EnKF with variational methods, several major operational NWP centers have implemented such approaches in their global data assimilation systems such as Environment and Climate Change Canada, Méteo-France, the European Center for Medium-Range Weather Forecasts, UK Met, Deutscher Wetterdienst (German Weather Service), Japan Meteorological Agency, and NCEP. Similar efforts for limited area data assimilation systems have also been tested.

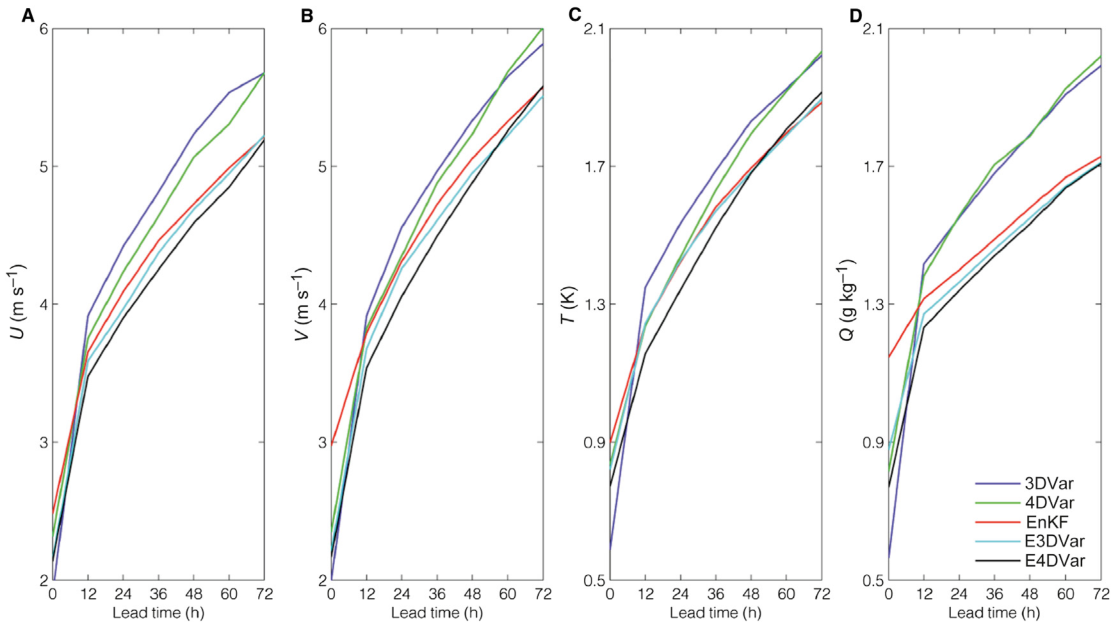

Fig. 3 Comparison between WRF-based 3DVar, 4DVar, EnKF, E3DVar, and E4DVar in terms of domain-averaged root mean square errors averaged over all 59 WRF forecasts from June 2003 for each Data Assimilation (DA) experiment at forecast lead times from 0 to 72 h evaluated every 12 h for (A) U (m s^{-1}), (B) V (m s^{-1}), (C) T (K), and (D) Q (g kg^{-1}). 3DVar, three-dimensional variation; 4DVar, four-dimensional variation; EnKF, ensemble Kalman filter. Adapted from Zhang, F., Zhang, M., Poterjoy, J., 2013. E3DVar: coupling an ensemble Kalman filter with three-dimensional variational data assimilation in a limited-area weather prediction model and comparison to E4DVar. Mon. Weather Rev. 141, 900−917. https://doi.org/10.1175/MWR-D-12-00075.1.

Summary

Ensemble-based data assimilation (EDA) has been more widely used in recent years due to its capability to use flow-dependent ('error-of-the-day') background error covariances, incorporate nonlinear model and observation operators, provide uncertainty estimations, and its ease to use and maintain. While it was first applied in convective-scale and mesoscale research, it is now adopted in many operational global models at major NWP centers, often hybrid with variational methods. It has been successfully used to assimilate different types of *in situ* and remote-sensing observations, including Doppler weather radar observations and satellite radiance observations. However, ensemble size used by most current EDA applications is too small, which leads to sampling errors and rank deficiency. While inflation and covariance localization techniques have been developed to combat sampling errors, more studies are still warranted to improve our understanding of their impacts and optimal use. Additionally, how to better treat model error, observation error, and nonlinearity and non-Gaussianity in real-world models and observations also deserve further studies.

References

Aksoy, A., 2013. Storm-relative observations in tropical cyclone data assimilation with an ensemble Kalman filter. Mon. Weather Rev. 141, 506−522.

Aksoy, A., Dowell, D.C., Snyder, C., 2009. A multicase comparative assessment of the ensemble Kalman filter for assimilation of radar observations. Part I: storm-scale analyses. Mon. Weather Rev. 137, 1805−1824.

Aksoy, A., Zhang, F., Nielsen-Gammon, J.W., 2006. Ensemble-based simultaneous state and parameter estimation with MM5. Geophys. Res. Lett. 33, L12801. https://doi.org/10.1029/2006GL026186.

Anderson, J.L., 1996. A method for producing and evaluating probabilistic forecasts from ensemble model integrations. J. Clim. 9, 1518−1530.

Anderson, J.L., 2009. Spatially and temporally varying adaptive covariance inflation for ensemble filters. Tellus 61A, 72−83.

Barker, D.M., Huang, W., Guo, Y.-R., Bourgeois, A.J., Xiao, Q.N., 2004. A three-dimensional variational data assimilation system for MM5: implementation and initial results. Mon. Weather Rev. 132, 897−914.

Caya, A., Sun, J., Snyder, C., 2005. A comparison between the 4DVAR and the ensemble Kalman filter techniques for radar data assimilation. Mon. Weather Rev. 133, 3081−3094.

Dowell, D.C., Zhang, F., Wicker, L.J., Snyder, C., Crook, N.A., 2004. Wind and temperature retrievals in the 17 May 1981 Arcadia, Oklahoma, supercell: ensemble Kalman filter experiments. Mon. Weather Rev. 132, 1982−2005.

Ehrendorfer, M., 2007. A review of issues in ensemble-based Kalman filtering. Meteorol. Z. 16, 795−818.

Evensen, G., 1994. Sequential data assimilation with a nonlinear quasi-geostrophic model using Monte Carlo methods to forecast error statistics. J. Geophys. Res. 99, 10143−10162.

Fujita, T., Stensrud, D.J., Dowell, D.C., 2007. Surface data assimilation using an ensemble Kalman filter approach with initial condition and model physics uncertainties. Mon. Weather Rev. 135, 1846−1868.

Gaspari, G., Cohn, S.E., 1999. Construction of correlation functions in two and three dimensions. Q. J. R. Meteorol. Soc. 125, 723−757.

Hamill, T.M., 2006. Ensemble-based atmospheric data assimilation. In: Palmer, T., Hagedorn, R. (Eds.), Predictability of Weather and Climate. Cambridge University Press, Cambridge, UK, pp. 124—156.

Hamill, T.M., Colucci, S.J., 1997. Verification of Eta—RSM short range ensemble forecasts. Mon. Weather Rev. 125, 1312—1327.

Honda, T., Amemiya, A., Otsuka, S., Lien, G.-Y., Taylor, J., Maejima, Y., Nishizawa, S., Yamaura, T., Sueki, K., Tomita, H., Satoh, S., Ishikawa, Y., Miyoshi, T., 2022. Development of the real-time 30-s-update big data assimilation system for convective rainfall prediction with a phased array weather radar: description and preliminary evaluation. J. Adv. Model. Earth Syst. 14, e2021MS002823.

Houtekamer, P.L., Mitchell, H.L., 1998. Data assimilation using an ensemble Kalman filter technique. Mon. Weather Rev. 126, 796—811.

Houtekamer, P.L., Mitchell, H.L., 2005. Ensemble Kalman filtering. Q. J. R. Meteorol. Soc. 131, 3269—3289.

Houtekamer, P.L., Zhang, F., 2016. Review of the ensemble Kalman filter for atmospheric data assimilation. Mon. Weather Rev. 144, 4489—4532. https://doi.org/10.1175/MWR-D-15-0440.1.

Jones, T.A., Stensrud, D.J., 2012. Assimilating AIRS temperature and mixing ratio profiles using an ensemble Kalman filter approach for convective-scale forecasts. Weather Forecast. 27, 541—564.

Jung, Y., Xue, M., Zhang, G., Straka, J.M., 2008. Assimilation of simulated polarimetric radar data for a convective storm using the ensemble Kalman filter. Part II: impact of polarimetric data on storm analysis. Mon. Weather Rev. 136, 2246—2260.

Kepert, J.D., 2009. Covariance localization and balance in an ensemble Kalman filter. Q. J. R. Meteorol. Soc. 135, 1157—1176.

Krishnamurti, T.N., Kishtawal, C.M., LaRow, T.E., Bachiochi, D.R., Zhang, Z., Williford, C.E., Gadgil, S., Surendran, S., 1999. Improved weather and seasonal climate forecasts from multimodel superensemble. Science 285, 1548—1550.

Le Dimet, F.X., 1982. A general formalism of variational analysis. CIMMS Rep. 22. Cooperative Institute for Mesoscale Meteorological Studies. 34 pp. [Available from: CIMMS, 815 Jenkins St., Norman, OK 73019.].

Leutbecher, M., Buizza, R., Isaksen, L., 2007. Ensemble forecasting and flow-dependent estimates of initial uncertainty. In: Proceedings of the ECMWF Workshop on Flow-dependent Aspects of Data Assimilation, Reading. ECMWF, United Kingdom, pp. 185—201.

Lorenc, A.C., 2003. The potential of the ensemble Kalman filter for NWP—a comparison with 4D-Var. Q. J. R. Meteorol. Soc. 129, 3183—3203.

Lynch, P., Huang, X., 1992. Initialization of the HIRLAM model using a digital filter. Mon. Weather Rev. 120, 1019—1034.

Meng, Z., Zhang, F., 2007. Tests of an ensemble Kalman filter for mesoscale and regional-scale data assimilation. Part II: imperfect model experiments. Mon. Weather Rev. 135, 1403—1423.

Meng, Z., Zhang, F., 2008. Tests of an ensemble Kalman filter for mesoscale and regional-scale data assimilation. Part III: comparison with 3DVar in a real-data case study. Mon. Weather Rev. 136, 522—540.

Meng, Z., Zhang, F., 2008. Tests of an ensemble Kalman filter for mesoscale and regional-scale data assimilation. Part IV: comparison with 3DVar in a month-long experiment. Mon. Weather Rev. 136, 3671—3682.

Meng, Z., Zhang, F., 2010. Limited-area ensemble-based data assimilation. Mon. Weather Rev. 139, 2025—2045.

Miyoshi, M., Kondo, K., Imamura, T., 2014. The 10,240-member ensemble Kalman filtering with an intermediate AGCM. Geophys. Res. Lett. 41 (14), 5264—5271.

Putnam, B.J., Jung, Y., Yussouf, N., Stratman, D., Supinie, T.A., Xue, M., Kuster, C., Labriola, J., 2021. The impact of assimilating ZDR observations on storm-scale ensemble forecasts of the 31 may 2013 Oklahoma storm event. Mon. Weather Rev. 149 (6), 1919—1942.

Shutts, G., 2005. A kinetic energy backscatter algorithm for use in ensemble prediction systems. Q. J. R. Meteorol. Soc. 131, 3079—3102.

Snyder, C., Zhang, F., 2003. Assimilation of simulated Doppler radar observations with an ensemble Kalman filter. Mon. Weather Rev. 131, 1663—1677.

Stratman, D.R., Yussouf, N., Jung, Y., Supinie, T.A., Xue, M., Skinner, P., Putnam, B.J., 2020. Optimal temporal frequency of NSSL phased array radar observations for an Experimental Warn-on-Forecast System. Weather Forecast. 35, 193—214.

Weisheimer, A., Doblas-Reyes, F.J., Palmer, T.N., Alessandri, A., Arribas, A., Déqué, M., Keenlyside, N., MacVean, M., Navarra, A., Rogel, P., 2009. ENSEMBLES: a new multi-model ensemble for seasonal-to-annual predictions—skill and progress beyond DEMETER in forecasting tropical Pacific SSTs. Geophys. Res. Lett. 36, L21711. https://doi.org/10.1029/2009GL040896.

Wang, C., Zhao, K., Zhu, K., Huang, H., Lu, Y., Yang, Z., Fu, P., Zhang, Y., Chen, B., Hu, D., 2021. Assimilation of X-band phased-array radar data with EnKF for the analysis and warning forecast of a tornadic storm. J. Adv. Model. Earth Syst. 13, 2020MS002441.

Xiao, Q., Sun, J., 2007. Multiple-radar data assimilation and short-range quantitative precipitation forecasting of a squall line observed during IHOP_2002. Mon. Weather Rev. 135, 3381—3404.

Zhang, F., Snyder, C., Sun, J., 2004. Impacts of initial estimate and observation availability on convective-scale data assimilation with an ensemble Kalman filter. Mon. Weather Rev. 132, 1238—1253.

Zhang, F., Weng, Y., Gamache, J.F., Marks, F.D., 2011. Performance of convection-permitting hurricane initialization and prediction during 2008—2010 with ensemble data assimilation of inner-core airborne Doppler radar observations. Geophys. Res. Lett. 38, L15810. https://doi.org/10.1029/2011GL048469.

Zhang, F., Weng, Y., Sippel, J.A., Meng, Z., Bishop, C.H., 2009. Cloud-resolving hurricane initialization and prediction through assimilation of Doppler radar observations with an ensemble Kalman filter. Mon. Weather Rev. 137, 2105—2125.

Zhang, F., Zhang, M., Poterjoy, J., 2013. E3DVar: coupling an ensemble Kalman filter with three-dimensional variational data assimilation in a limited-area weather prediction model and comparison to E4DVar. Mon. Weather Rev. 141, 900—917. https://doi.org/10.1175/MWR-D-12-00075.1.

Zhang, Y., Sieron, S.B., Lu, Y., Chen, X., Nystrom, R.G., Minamide, M., Chan, M.Y., Hartman, C.M., Yao, Z., Ruppert Jr., J.H., Okazaki, A., 2021. Ensemble-based assimilation of satellite all-sky microwave radiances improves intensity and rainfall predictions for Hurricane Harvey (2017). Geophys. Res. Lett. 48, 2021GL096410. https://doi.org/10.1029/2021GL096410.